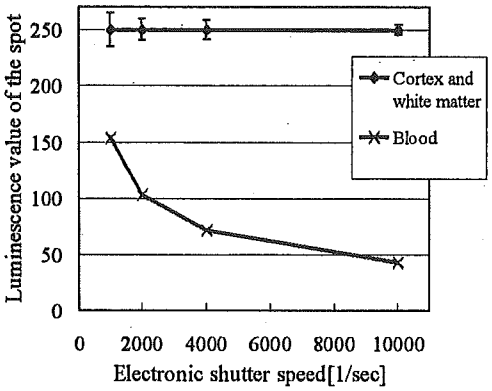

Fig. 5. Difference in the luminance value of the spot by the irrigated object.

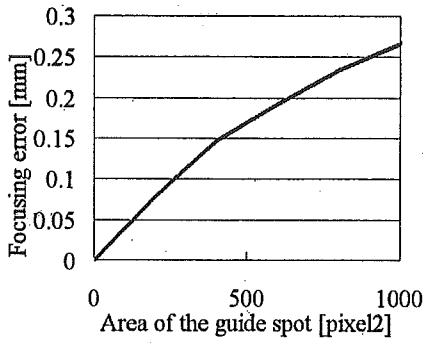

Fig. 6. Relationship between the error and the area of the extracted spot.

matter, or blood. We examined the relationship between target tissues and spot extraction. From this pilot study, we developed an appropriate spot extraction method for biomedical tissues.

A. Spot Extraction Issues

Fig. 5 shows the differences in the luminance values of the spot according to the object irrigated. The horizontal axis is the electronic shutter speed of the CCD camera and the vertical axis is the luminance value of the spot. The tested objects were porcine cortex and white matter, and rat blood. Extraction of the spot was difficult in blood compared with brain parenchyma. To extract the spot successfully, it was necessary to lower the threshold in blood. On the other hand, if the threshold was too low, noise occurred, and extraction of the spot became impossible.

This system determines the coordinates of the spot by measuring its center of gravity. These coordinates contain error caused by penetration of the biomedical tissue. This is because the camera catches the light from the inside of the tissue. Fig. 6 shows the relationship between the error and the area of the extracted spot. The test was performed on a phantom of Intralipid-10% [6], [7]. Its scattering coefficient at the wavelength of 532 nm was 3 cm^{-1}, which is near the value of gliomas [5]. If the area of the spot was large, the error increased.

B. Threshold Control

If a luminance threshold is fixed to a high level, for a target such as blood it was impossible to extract the spot in some conditions. However, if the luminance threshold is low, the area of the spot becomes large, and then the error becomes larger. It is desirable to control the luminance threshold to an appropriate value, so that the area of an extracted spot is constantly small. We developed a threshold controlling method based on the relationship between the luminance threshold and the area of an extracted spot.

We used a single mode fiber for the green guide laser with a wavelength of 532 nm. Its light intensity distribution depends on the normal distribution. If a target has only isotropic back scattering and no laser penetration efficiency, the relationship between light intensity and the distance from the center of a laser spot is (1).

$$I \approx \exp\left(-d^2/2\sigma^2\right)/\sqrt{2\pi}\,\sigma \tag{1}$$

where

I = light intensity,
d = distance from the center of a laser spot,
σ = standard deviation of the distribution.

Although the laser penetrates into brain tissues, the relationship between light intensity and the distance from the center of a laser spot is similar to (1). The relationship between the luminance threshold and the area of an extracted spot was derived from (1). The luminance threshold corresponds to light intensity and the area of an extracted spot corresponds to the square of the distance from the center of a laser spot (2).

$$Y = a\exp(-bA) + c \tag{2}$$

where

Y = luminance threshold,
A = area of spot,
a, b, c: constants—dependent on the target conditions.

Fig. 7 shows the relationship between the luminance threshold and the area of an extracted spot, and a curve approximated from (2) for white matter. The values of a, b, c differ according to the target tissue conditions. These three numbers were obtained with the luminance threshold Y, the area of an extracted spot A, and a histogram of luminance levels as follows:

1) A histogram of luminance levels was taken for a color image before binarization.
2) c is the asymptotic value of the luminance threshold. We determined it as the value 40% from the top of the histogram, where the area of the spot exponentially increased.

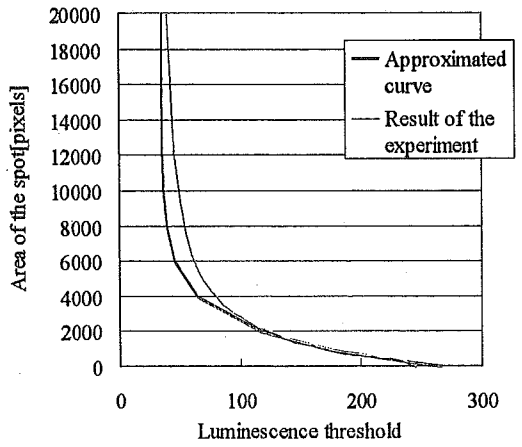

Fig. 7. Relation between the luminance threshold and the area of the extracted spot and an approximated curve in white matter.

3) At the peak value of the histogram, Y_{max}, the area of the spot $A = 0$. a was determined as follows: (3)

$$Y_{\max} - c = a\exp(-b \times 0) = a \tag{3}$$

4) Then b was determined from Y and A (4).

$$b = -\ln((Y - c)/a)/A \tag{4}$$

When focusing, the approximated function was calculated using the above method for every process. We could assume the appropriate value of the luminance threshold used in the next process by this approximated function. The method of controlling the luminance threshold was as follows. Before focusing, A_0 was set as the desired value of the area of the spot: sufficiently small to reduce the error due to penetration.

0) Focusing started.
1) The area of a spot, A_n, was obtained with the luminance threshold Y_n.
2) The approximate function for the relationship between Y_n and A_n was calculated (5).

$$Y_n = a_n \exp(-b_n A_n) + c_n \tag{5}$$

3) Y_{n+1} was computed as follows (6), and used for the next process.

$$Y_{n+1} = a_n \exp(-b_n A_0) + c_n \tag{6}$$

4) Return to 2).

As the device is moving at a speed of 2–4 mm/sec and the target tissue is being ablated while focusing, the condition of the target tissue is changing with time. Therefore, the assumed value of the threshold based on the current process is not perfectly adapted to the next process. However, the operating period of this system is 50 ms and the distance moved during this period is 0.1–0.2 mm, and thus the conditions of the target may not differ much in each consecutive process. Therefore, this method may be sufficient to allow stable extraction of the laser spot. In the following chapter, we compared this method with a method using a fixed threshold.

IV. Experiment

The experiments evaluating positioning accuracy, following error, and the threshold control methods are described in this chapter. These experiments were performed without ablation with the micro laser. Tests in combination with the micro laser will be performed in the future.

A. Experimental Evaluation of Positioning Accuracy

As an initial point, a focal point for the device was set on the horizontal target plane. The device was then moved vertically ± 0.4 mm from the focal point. Focusing was performed, and we measured the positioning error.

The average of the results was 0.04 mm, with a standard deviation of 0.05 mm, results fulfilling the desired specifications. The positioning accuracy of the stepping motor used in this system is 0.02 mm. The resolution based on the resolution of the CCD camera is 0.024 mm. These were considered as the main factors in the error.

B. Experimental Evaluation of the Following Error

The following error was measured for ascending and descending slopes. The angle of the slope was 45 degrees. Focusing was performed to the slope in a vertical direction. The device moved horizontally at a constant speed of 1, 2, 4, and 6 mm/sec. The distance moved was 10 mm.

The device followed the slope with constant delay at any traveling speed. There was no significant difference between ascending and descending slopes. The delay increased in proportion to the traveling speed (Fig. 8). These results fulfilled the desired specification of 0.5 mm.

C. In Vitro Threshold Control

We compared the method of dynamically changing the

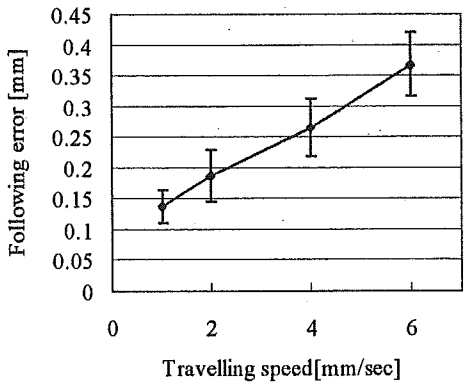

Fig. 8. Average of the following error with each traveling speed.

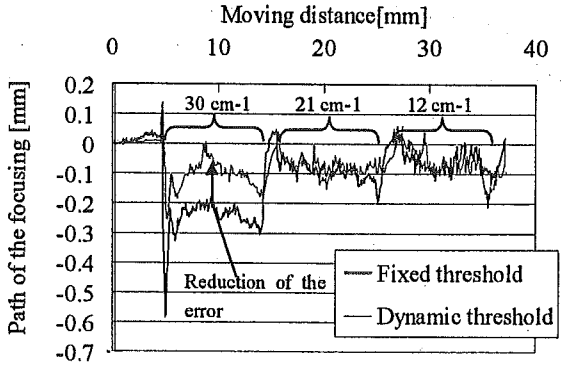

Fig. 9. Paths of the device *in vivo* experiment. The blue line is the path with the fixed threshold. The red line is the path with the dynamically changed threshold.

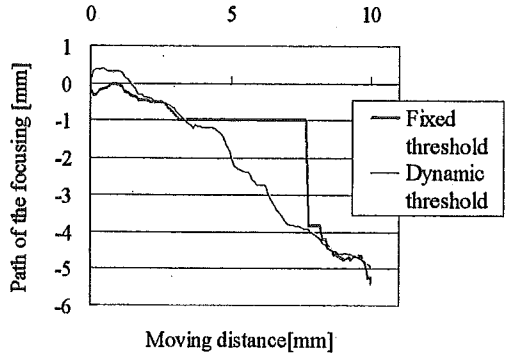

Fig. 10. Paths of the device *in vitro* experiment. The blue line is the path with the fixed threshold. The red line is the path with the dynamically changed threshold.

TABLE I
AVERAGE AND STANDARD DEVIATION OF THE AREA OF THE EXTRACTED SPOT.

		Method of the Threshold	
		Fixed	Dynamic
Area of the extracted spot [pixel]	Average	463	48
	Standard deviation	111	46

TABLE II
AVERAGE AND STANDARD DEVIATION OF THE AREA OF THE EXTRACTED SPOT AND THE SUCCESS RATE OF THE SPOT EXTRACTION.

		Method of the threshold	
		Fixed	Dynamic
Area of the extracted spot [pixel]	Average	101	78
	Standard deviation	102	62
Spot acquisition rate [%]		30	100

luminance threshold with a method using a fixed threshold. The device was consecutively moved on a phantom composed of Intralipid-10% [6], [7] with three different scattering coefficients, aligned in the order of 30, 21, and 12 cm^{-1} at the wavelength of 532 nm. The coefficient of 30 cm^{-1} is similar to that of white matter [5]. The width of each part was 10 mm and the interval between the parts was 1 mm. Focusing was performed using the two methods. The velocity of the device was 2 mm/sec horizontally. In the method of controlling the threshold, the desired value of the spot area A was set to 50 pixels. The luminance threshold was set to 100 in the fixed threshold method.

The paths of the device are shown in Fig. 9. The error was minimal on the 30 cm^{-1} part; reduced to 0.14 mm on average with the dynamically changing method. The area of the extracted spot was smaller and less variable with the dynamically changing method (Table I). As the spot was rather large and luminous on the 30 cm^{-1} part, this method worked most effectively.

D. In Vivo Threshold Control

Two methods for luminance thresholding were evaluated in *in vivo* experiments. The target was the surface of a porcine brain exposed by craniotomy under anesthesia. Focusing was performed while moving 10 mm horizontally at 2 mm/sec. In the method controlling the threshold, a desired value of the spot area A was set to 50 pixels. The luminance threshold was set to 100 in the fixed threshold method.

Fig. 10 shows the paths of the device. In the middle of the line, it was impossible to extract the guide spot using the fixed threshold method. Table II shows the data related to the extracted spots as the average and standard deviation of the area of the spots and the success rate of the extraction. Although the success rate of the fixed threshold method was only 30%, that of the controlling threshold method was 100%. Although the two lines in Fig. 10 indicate the same line on the porcine brain, they do not coincide. It is assumed that the reason for the difference was pulsation of the brain surface.

V. DISCUSSION AND CONCLUSIONS

We have developed a compact automatic-focusing system for micro laser instruments for neurosurgery. The wavelength of this laser is 2.8 μm and the laser is used for precise ablation of brain tumors. In this system, position

measurement was performed using a triangulation method with a guide laser and a small CCD camera. A surgeon can identify the treated point by looking at the guide laser. As the mechanism is rather simple, it was easy to realize a compact device.

The light radiated onto biomedical tissues is attenuated and penetrates the tissue according to its scattering and absorption features. According to the condition of the target, the appropriate value for each measurement parameter was different. For example, it was necessary to appropriately control the luminance threshold in the image processing, and we developed a new technique for controlling the threshold.

The positioning accuracy and the following error of this system were evaluated. The results fulfilled the desired specifications.

The methods of controlling the threshold and using a fixed threshold were compared. In *in vitro* experiments, the error when controlling the threshold was less than when using the fixed threshold. In *in vivo* experiments, the error was also reduced, and the success rate of the spot extraction improved greatly. The threshold controlling method effectively worked for biomedical tissue.

The evaluations performed in this paper did not consider the pulsation of the brain surface. As it is assumed that the human brain has a certain amount of the pulsation, it is necessary to evaluate the effects of pulsation on following error.

In the future, we will perform tests in combination with the ablation laser to achieve a precise system for operation upon brain tumors.

ACKNOWLEDGMENT

We wish to thank many people and groups who have contributed to this effort. One of them deserving special mention is Yasuo Oda of chief engineer of Biomedical Precision Engineering Laboratory, the University of Tokyo. The research funds was based in part on Grant-in-Aid for Scientific Research of JSPS (# 15700349) and Terumo Lifescience Foundation.

REFERENCES

[1] T. Maruyama, et al, "Intraoperative detection of malignant gliomas using 5-Aminolevulinic acid induced protoporphyrin fluorescence, openMRI and real-time navigation system," Computer Assisted Radiology and Surgery, vol. 15, pp. 270-275, 2001.

[2] K. Shimizu, et al, "Application of blue semiconductor laser to measurement of 5-ALA induced fluorescence for intraoperative detection of brain tumor," Proceedings of 6th Japan-France Congress on Mechatronics and 4th Asia-Europe Congress on Mechatronics, 2003, pp. 135-140.

[3] S. Omori, Y. Muragaki, I. Sakuma, and H. Iseki, "Robotic laser surgery with λ = 2.8um microlaser in neurosurgery," Journal of Robotics and Mechatronics, vol. 16, no. 2, pp. 122-128, 2004.

[4] S. Omori, R. Nakamura, Y. Muragaki, H. Iseki, K. Takakura, Improvement study of computer controlled mid-infrared laser system for neuro-surgery, Proceedings of 13th conference of Japan Society of Computer Aided Surgery (JSCAS), pp. 37-38, 2004

[5] Sterenborg HJ, et al, "The spectral dependence of the optical properties of the human brain," Lasers Med Sci, vol. 4, pp. 221-227, 1989.

[6] "Optical properties spectra," http://omlc.bme.ogi.edu/spectra/.

[7] J. van Staveren, J. M. Moes, J. van Marle, A. Prahl, J. C. van Germert, "Light scattering in Intralipid-10% in the wavelength range of 400-1100 nm," Appl Opt, vol. 30, pp. 4507-4514, 1991.

2005 IEEE/RSJ International Conference on Intelligent Robots and Systems

Compact Forceps Manipulator for Laparoscopic Surgery*

Takashi Suzuki, Youichi Katayama, Etsuko Kobayashi, Ichiro Sakuma
Graduate School of Frontier Sciences, The University of Tokyo
7-3-1, Hongo, Bunkyo-ku, Tokyo, Japan
{*t-suzuki, katayama, etsuko*}*@miki.pe.u-tokyo.ac.jp, isakuma@k.u-tokyo.ac.jp*

***Abstract*— Forceps manipulating robots have been developed for assisting surgeons to realize high-quality and precise operation in laparoscopic surgery. Currently several commercially available systems greatly contributed to operations. Still their large size causes problems in the operating theater, thus they need to be miniaturized. We developed a new compact forceps manipulator. It consists of two parts; friction wheel mechanism which rotates and translates the forceps ($62\times52\times150$[mm^3], 0.6[kg]), and gimbals mechanism which drives the forceps around the incision hole on the abdomen to determine the direction of forceps ($135\times165\times300$[mm^3], 1.1[kg]). Thus, the four DOF motion of forceps in laparoscopic surgery was realized. Ultrasonic motor was adopted for actuating friction wheel mechanism because of its small size, high torque and cleanliness. We controlled the manipulator in semi-closed loop using rotary encoders. Mechanical evaluation results showed that feedback loop control and compensation of control command improved the positioning accuracy. Positioning accuracy of the gimbals mechanism was less than 0.6 [deg], and that of friction wheel mechanism was less than 0.2 [mm] in translation and 1 [deg] in rotation. *In vitro* experiment simulating usage in the clinical environment revealed that this manipulator realized stable motion even if the liquid materials such as blood attached onto the forceps. The new manipulator was promising and useful in laparoscopic surgery.**

***Index Terms*— Minimally invasive surgery, surgical robot, friction wheel, gimbals mechanism, ultrasonic motor.**

I. Introduction

Laparoscopic surgery is widely performed as a means of minimally invasive surgery. In this method, surgeons make 3 - 4 holes on the abdominal wall, and entire operations are conducted inside the abdominal cavity through the holes using rigid thin scope and long-handled surgical tools such as forceps, scalpel (Fig. 1(a)). Compared with the conventional laparotomy that requires large incision on the abdomen, laparoscopic surgery has benefits for patients because of its small invasion; reduction of postoperative pain, discomfort, medication, and time needed for recovery. It has, however, some difficulties for surgeons. Forceps have the limited Degrees of Freedom (DOFs) (two DOFs for orientation of forceps, two DOFs for insertion and rotation of forceps), and limited DOFs reduce the dexterity of the surgeon (Fig.1(b)). As the surgical instruments are bound at the incision hole, procedure is operated symmetrically around the incision hole, so that surgeon gets confused. Thus, this technique requires great skill, resulting in physical and mental stress for surgeon. Responding to these drawbacks, surgery-assisting robots have been developed for thoracic and abdominal surgery [1], [2], [3], [4], [5]. Some systems, such as da Vinci$^{(R)}$, are clinically applied and commercially available. These robots enhanced the dexterity and ability of surgeons, which contributed to the higher-quality and more precise operation that could not be realized using conventional forceps. Some of them, however, have problems arising from their size [6], such as;

– Large size for conventional operating theaters.
– Operating space above the abdomen is occupied by the manipulator.
– Collision with manipulators or surgeons.

Thus, a new compact surgery assisting robot is required [3].

We have developed a compact forceps manipulator using "friction wheel mechanism" (FWM)[7] and "gimbals mechanism". The FWM realizes the axial translation of the forceps. Ikuta et al [8] used the same kind mechanism for the axial translation and rotation of the colonoscope in the virtual endoscope system. Gimbals mechanism has two rotational axes inside it and inclines freely in all directions, that provides the pivoting motion of forceps. This manipulator works to drive robotized forceps [5], [9], [10], [11]. As

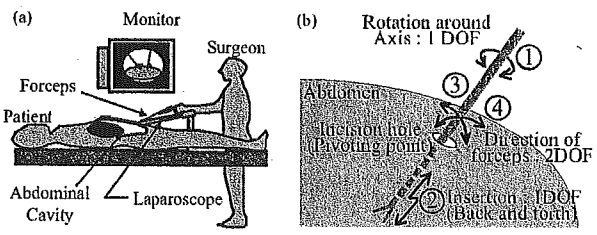

Fig. 1. Laparoscopic surgery; (a) Surgeons operate forceps (long-handled surgical tools) watching the view from laparoscope (thin camera penetrated into the abdominal cavity). (b)Limited degrees of freedom of the forceps. Instruments are bound at the incision hole, thus surgeons operate them symmetrically around it. Each DOF indicated with circled number 1 – 4 corresponds to numbering in Fig.3.

*This work is partially supported by "Research for the Future Program (JSPS-RFTF 99I00904)" funded by Japan Society for the Promotion of Science, Electro-Mechanic Technology Advancing Foundation, "Research and Development of the Compact Surgical Robot System for Future Medical Care" funded by New Energy and Industrial Technology Development Organization (NEDO), and "Research on medical devices for analyzing, supporting and substituting the function of human body" funded by Ministry of Health, Labour and Welfare.

for the input method, we can use both numerical control system based on computer assisted surgical planning and master manipulator in a master-slave system with different configuration.

In the former study, a prototype was manufactured, and feasibility was shown as a forceps manipulator [12]. At the same time, some problems emerged. The rotational motion of the ultrasonic motor we adopted for actuation was affected by temperature and load, and the speed of rotation varied depending on various factors. In accordance with the unstable motion of the actuator, the motion of forceps was also unstable [13]. The low machining accuracy, especially in FWM, also affected the unstable motion of the forceps.

In this study, we have developed a new prototype using miniaturized ultrasonic motors with rotary encoder and DC servomotors. We report 1) improvement of machining accuracy to provide stable operation, 2) feedback control system using pulse signal from the rotary encoders, 3) mechanical performance evaluation. Lastly we conducted *in vitro* experiments considering the clinical application.

II. Method

A. Specification requirements

We set the following requirements for the manipulator.
- The manipulator must be miniaturized enough that at least three sets can be installed in the operating field, that correspond to both hands of surgeon and one hand of assistant.
- The system should be attached to the bedside like ZEUS system [14] for easy setup and easy detachment.
- The manipulator provides the four DOFs shown in Fig. 1(b).
- The system has enough power and moving range. It can bear 4[N] of weight considering the one third of liver weight (whole liver is approximately 1.2 [kg]), and cover the whole liver (Fig. 2).
- Positioning accuracy is less than 1[mm] and 1[deg] to realize precise operation.

As for the mechanical performance such as speed, torque, force, and accuracy, they depend on the intended organ, surgical procedure, and so on. Especially in the case of image-guided surgery, the resolution of the imager defines the accuracy required to the manipulator. In this study, we set above values assuming that cholecystectomy is conducted by this manipulator.

B. System configuration

To satisfy the abovementioned requirements, we adopted following two mechanisms; "Friction wheel mechanism" (FWM) realizes the rotation around the forceps shaft, and translation along the shaft (circled number 1 and 2 in Fig.3). Gimbals mechanism is used to determine the direction of the forceps (3 and 4 in Fig.3). We set this manipulator above the incision hole. This is because mechanisms and actuators should be mounted near the operating field so that they require less torque or force and miniaturization of them are realized [3].

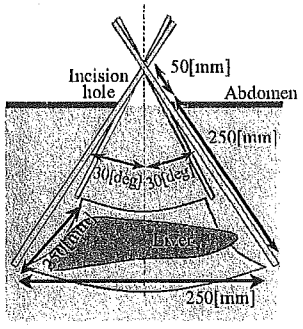

Fig. 2. Forceps working space covers the whole liver. We assumed the area (250 × 250 [mm^2]) from the size of normal Japanese male.

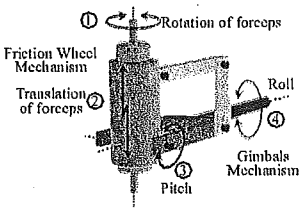

Fig. 3. System configuration. Rotation and translation are realized by friction wheel mechanism. Gimbals mechanism drives the forceps around the incision hole to determine the direction of the insertion.

1) Friction wheel mechanism (FWM):

a) Friction wheel: We used "friction wheel". It consists of three titled idle rollers and outer case (Fig. 4(a)). Among the three rollers, we insert the forceps, and rollers hold the shaft of forceps. When outer case rotates, rollers travel spirally on the shaft of forceps (Fig. 4(b)) [15]. We have two kinds of FWM with different tilting angle. They are like right-handed screw and left-handed one. Each mechanism makes spiral motion in each direction. We combine the two motions to realize rotation and translation (Fig. 4(c)). The tilt angle was set at 30 [deg] in this study. We adopted an ultrasonic motor with rotary encoder (custom order, Fukoku, Japan) to drive the outer case of friction wheel because it has advantages in compact size, light weight, high holding torque, and suitable for hollow-shaft one.

b) Rotation: For the rotation of the forceps around its shaft, we rotate both friction wheels in the same direction. In this case, rollers holding the shaft do not rotate, and do not make spiral motion. Thus, the shaft held by rollers rotates at the same speed as the FWM (Fig.5(a)).

c) Translation: In the case of translation, we rotate each FWM in the opposite direction (Fig.5(b)). Each rotational motion cancels each other, and only translation remains. Thus translation along its shaft is realized.

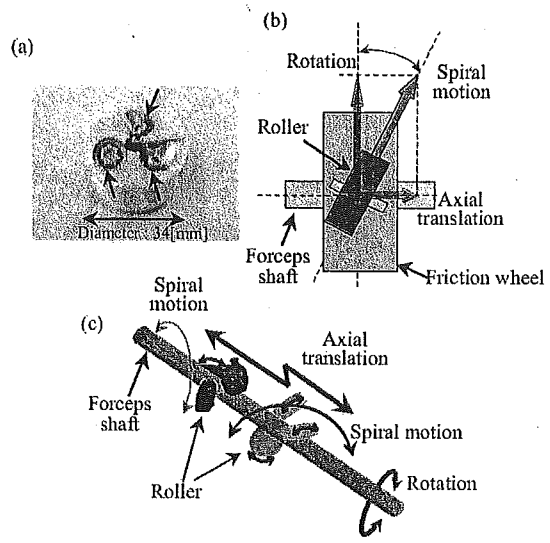

Fig. 4. Friction wheel mechanism; (a) a FWM has three rollers (arrow). (b) Roller tilted at a certain degrees. When friction wheel rotates around the forceps shaft, rollers travel spirally on the surface of shaft. That motion can be divided into two motions; axial translation along the shaft and rotation around the shaft. (c) We use two kinds of FWM with different tilting angle. We combine two spiral motions to realize rotation and translation.

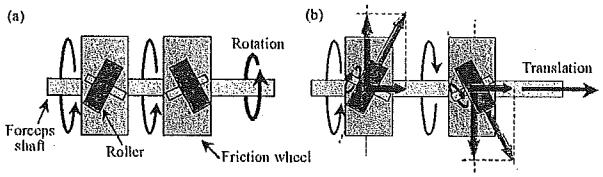

Fig. 5. Driving mechanism of forceps;(a) Rotation. (b) Translation.

In the former prototype, because of the low machining accuracy, each center of friction wheels was not located in the same straight line, thus, FWM did not move smoothly. In this study, we modified the housing where friction wheels were mounted, and arrayed each center of friction wheels in the same line. Because the rotational speed of ultrasonic motor was not stable depending on the load, we implemented optical rotary encoder to get the rotational speed information.

2) Gimbals mechanism: Gimbals mechanism has merits in its compactness and wide working range. The axes of two rotational motions cross at one point and it simplifies the control algorithm. In many study (ex,[1], [2]), it is said that the remote center of motion (RCM) must be located at the incision hole. Gimbals mechanism, however, has its rotational center inside it, not at the incision hole. As we reported in [12], it is not a problem because abdominal muscle of a patient under anesthesia gets relaxed, and manipulator will not damage the abdominal wall by driving the forceps. The rotational center is located above the trocar at the incision hole.

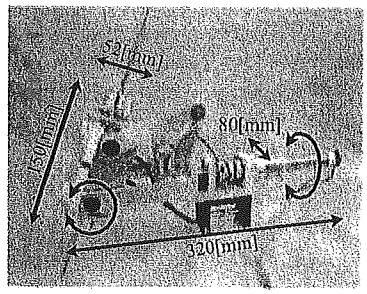

Fig. 6. New prototype. Weight is 1.7 [kg].

We newly implemented DC servomotors (ENC-185801-1000/3CH-SAP1/576, Chiba Precision Co.,Ltd, Japan) for actuation. This motor has the special controller unit that simplifies the building up of closed feedback loop. The motor for pitch motion was located at some distance from the incision hole, and linkage mechanism was added for transmission (circled number 3 in Fig.3). We intended to keep sterilization around incision hole by separating sterilized and nonsterilized part via linkage mechanism. Linkage mechanism also works as a mechanical stopper to limit the working range of pitch for safety.

C. New prototype

The new prototype is shown in Fig. 6. Weight is 1.7 [kg]. FWM was $62\times52\times150[mm^3]$, 0.6[kg], and gimbals mechanism was $135\times165\times300[mm^3]$, 1.1[kg].

III. Evaluation Experiments

A. Mechanical performance evaluation

We conducted mechanical performance evaluation of our new prototype. Torque of pitch, roll, and rotation, and force of translation were measured by 6-DOF strain gauge force/torque sensor (MINI sensor 8/40, BL Auto Tech, Japan). We repeated the measurements for twenty times, and calculated the average and standard deviation. We also measured the working range of each axis, and maximum driving speed without load. Digital microscope (VH-7000C, KEYENCE, Japan) was used for measurement of working range, and its measurement resolution was 0.1[mm] and 0.5[deg]. We used video camera to measure the speed. In pitch and roll of gimbals mechanism, acceleration and deceleration time was 100 [ms] respectively. As for the rotation and translation of FWM, we cannot control the acceleration and deceleration time of the ultrasonic motor because of its specification, and we measured average speed. Measurements were repeated ten times for gimbals mechanism, twenty times for FWM.

TABLE I

RESULTS OF MECHANICAL PERFORMANCE EVALUATION

	Torque/Force	Speed	Working range
Pitch	4.60±0.19[Nm]	5.0[rpm]	-35.0–+37.0[deg]
Roll	3.76±0.20[Nm]	5.0[rpm]	±180.0[deg]
Rotation	$6.3\pm0.9\times10^{-2}$[Nm]	41.8±0.6[rpm]	no limitation
Translation	61.0±0.7[N]	6.5±0.1[mm/s]	no limitation

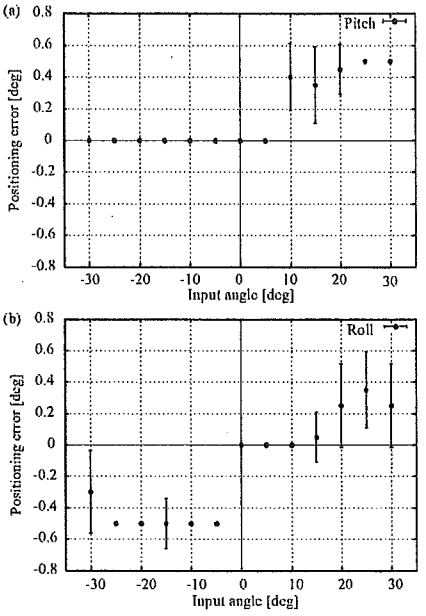

Fig. 7. Evaluation results of positioning accuracy; (a) pitch (b)roll.

Results are shown in Table.I. As for the rotational torque of FWM, the diameter of forceps model used in this evaluation was 5 [mm], thus the FWM can lift up the weight of 25.2±3.6[N] by rotating the forceps. Though the translation force seemed excessive, big force is required for the quick response. It does not mean that this manipulator always works with the maximum force. The working ranges of rotation and translation have theoretically no limitation, however, the translation range is restricted by the length of forceps and rotational range will be restricted by the arrangement of electric wires of the robotized forceps integrated into this manipulator.

B. Positioning accuracy of gimbals mechanism

We measured the positioning accuracy of gimbals mechanism at every 5 [deg] from -30 [deg] to +30 [deg]. Measurements were conducted twenty times for pitch and roll respectively. Fig. 7 shows the relation between input angle and positioning error.

C. Positioning accuracy of friction wheel mechanism

1) Stable motion by separation of rotation and translation: As mentioned in III.Method, translation and rotation of the forceps were realized using a couple of FWM. If each spiral motion generated by friction wheel is completely the same as each other, translation and rotation are realized without error motion. that is, we can realize no rotational error in translation, and no translation error in rotation. Similar issue was discussed in [8].

Thus, we controlled the ultrasonic motor to match the rotation speed using signal from rotary encoder. However, the motion of forceps was not stable. It was caused by the fact that each spiral motion differs slightly because of machining and manufacturing error even though the rotation speed matches completely.

Finally, we adopted compensation element based on the results of measurements in the control algorithm. When we input 45 [mm] translation command (which corresponds to 1800 [deg] rotation of friction wheel), forceps rotated 14.5 [deg]. This shows rollers of one friction wheel travels longer distance, and those of the other shorter by the angle of 14.5 [deg]. We applied two coefficients; 1 - (14.5 / 1800) to longer travelling one, and 1 + (14.5 / 1800) to shorter travelling one.

We measured the amount of translation error when rotation command of 10 revolutions was input. We also measured the amount of rotational error when translation command of 50 [mm] was input. As the measuring instrument, we used digital microscope. In Table.II., we compared the error of forceps motion. Comparing first and second line, new prototype realized more stable motion than old one. This means redesign of manipulator works well. Also, comparing second and third line, compensation leads to successful outcome.

2) Positioning accuracy evaluation: We measured the positioning accuracy of FWM. In the rotation, input command varied from -180 [deg] to +180 [deg], and measurements were conducted every 45 [deg]. In the translation, input command changes from -70 [mm] to +70 [mm], and we measured every 20 [mm]. Measurements were repeated twenty times respectively. In this evaluation, abovementioned compensation method was used. The results are shown in Fig. 8

D. Positioning error in slip

FWM uses rolling friction force to drive the forceps. Considering the clinical use in the operating theater, liquid

TABLE II

COMPARISON OF MOTION ERROR BETWEEN PROTOTYPES

	Rotation [mm]	Translation [deg]
Old prototype	0.1 ± 0.1	27.8 ± 10.4
New prototype	0.0 ± 0.0	14.5 ± 2.9
Compensation	0.0 ± 0.0	1.1 ±1.1

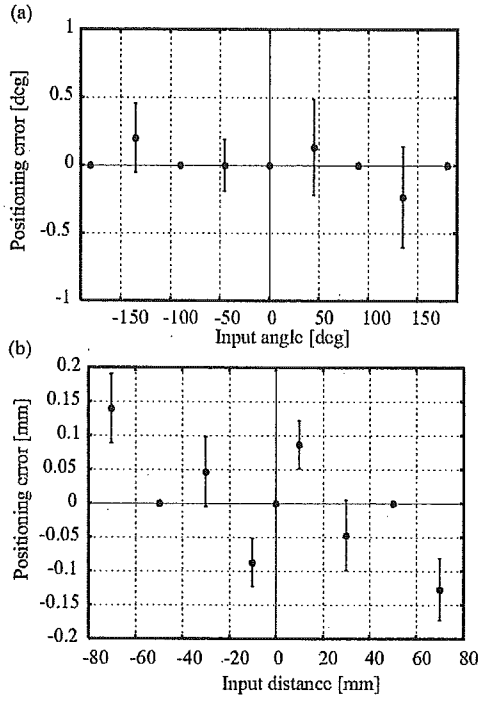

Fig. 8. Evaluation results of positioning accuracy. (a) rotation (b) translation.

matter such as blood might attach onto the surface of forceps, so that the friction force between rollers of FWM and forceps shaft will change, and slip will occur. In out prototype, we use rotary encoder mounted on the ultrasonic motor for semi-closed feedback loop. Once slip occurs, the system will lose the position of the forceps.

Thus, we conducted *in vitro* evaluation simulating clinical use of forceps. Forceps shaft was set in vertical direction, and coated with blood of rat. We added heparin for the anticoagulation of blood. As the result, even when 2 [kg] weight (five times larger than the requirements) was attached at the distal end of forceps, slip did not occur. The photograph of forceps shaft is shown in Fig. 9. From the spiral trajectory on the surface of forceps shaft, we can think that the rollers inside FWM wipe out the blood according to the rotation of FWM.

IV. Discussion

A. Forceps manipulator

1) Friction wheel mechanism (FWM) : Redesign of manipulator and compensation element in the control algorithm improved the stability of the motion. The requirements for positioning accuracy was satisfied. It is remarkable in the reduction of rotation error of translation. Although the

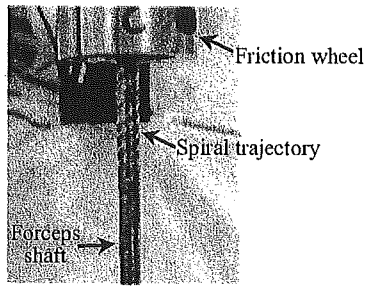

Fig. 9. Spiral trajectory on the surface of forceps. Rollers wiped out the blood on the surface.

compensation element was calculated from the limited measurement results, the machining and manufacturing error does not change depending on the input command, thus the compensation technique can be applied to total working range.

The biggest advantages of FWM are that it does not have mechanical limitation of the working range, and that it realize both rotation and translation with one mechanism. In the case that we drive something like forceps along its longitudinal axis, ball screw can be given as a typical example of linear actuator. While it has merits in high positioning accuracy, high rigidity, and fast motion, the problem is the thread part of the screw. The longitudinal dimension of the manipulator increases by the length of the ball screw. Longer arm requires higher torque and bigger motor, so that manipulator might upsize. Additionally, as thread part of most ball screw need grease, it cannot be washed and sterilized, and must be covered with surgical drape. Thus, ball screw is not always appropriate to surgical device. On the other hand, our friction wheel mechanism uses the shaft of forceps directly for driving, and needs no extra length and attachment part. This miniaturizes the manipulator.

2) Gimbals mechanism: As a mechanism to determine the direction of forceps, we eliminated the RCM mechanism and adopted the gimbals mechanism to realize a compact manipulator. Measured working space met the requirements. Excessive wide working space, however, may raise a problem. In this study, safety mechanism to limit the pitch was implemented. We are going to adopt the same fashion to the roll.

As the results of implementing DC servomotors, the positioning accuracy of gimbals mechanism satisfied the requirements, however, the gimbals' maximum positioning error of 0.6 [deg] corresponds to 2.6 [mm] error at the tip of 250 [mm] long forceps. This means that it did not meet the requirements of less than 1[mm]. With shorter than 95 [mm] long forceps, requirement (less than 1[mm]) will be satisfied.

3) Clinical application: As the results of *in vitro* experiments, slip between rollers and forceps did not occur

when blood attached onto the surface of forceps. The spiral trajectory on the surface of forceps (Fig.9) shows that rollers and forceps are contiguous so closely that blood on the surface is wiped out. Slip, however, occurred after blood on the surface got dried. This is probably because only wet blood can be wiped out, but blood clot like a thing coating on the surface cannot. Thus the blood should be swept away by physiological saline or wiped off by a scraper before clotting.

The area occupied by a set of manipulator on the abdomen was 12,000(=80×150) [mm^2]. This is compact size enough to install three sets of this manipulator, which corresponds to both hand of surgeon and on hand of assistant.

B. Future works

In our prototype, the position of the forceps was calculated from the rotation number of the ultrasonic motor as a semi-closed loop system. As discussed above, required positioning accuracy and nonslip operation were realized. However, for realization of more precise operation, we will make closed loop and realize feedback control system by sensing the position of forceps directly. As examples of sensing devices, we are now considering a commercially produced optical-tracking system (ex. Polaris$^{(R)}$, Northern Digital Inc., Canada) or magnetic position sensor (ex. microBIRD^{TM}, Ascension Technology Corporation, USA). Though they have shown the good performance in operation room, it is known that optical system does not work when the markers get behind objects, and it is also known that magnetic sensor can be affected by the metal material in the operating room, such as surgical table, instruments. Thus we have to choose sensing device carefully. Alternatively, we have another choice to develop a new sensing device like an optical mouse. Inside a optical mouse, image sensor takes hundreds of images per second and compares the two images, then the difference of the images shows the direction and the distance of motion of the mouse. In a similar fashion, the surface texture of the forceps can be taken by image sensor mounted on the manipulator, and motion can be calculated from the difference between each image.

As another work, we will also modify our forceps manipulator as a sterilization-compatible one for clinical application. Technical problem in current prototype is sterilization of bearing which works as a roller and ultrasonic motor for friction wheel mechanism, DC motor for gimbals mechanism. Bearing can be changed for greaseless one that uses plastic material for sliding surface. As for ultrasonic motor, water-proof packaging can be applied using sealing materials and O-ring. Thus, we will be able to sterilize the whole body of FWM. DC motor for gimbals mechanism can be replaced by sterilization-compatible motor commercially available for food and chemical industry. More especially, we can implement an easily detachable transmission mechanism between motors and mechanical moving parts. This method, at the same time, realizes the separation of sterilized and nonsterilized part [16], and realizes a safety mechanism by detaching the transmission part in the case of malfunctions.

V. Conclusion

In this study, we developed a compact forceps manipulator for laparoscopic surgery. It consisted of friction wheel mechanism for rotation and translation of forceps (62×52×150[mm^3], 0.6[kg]), and gimbals mechanism for determining the direction of forceps(135×165×300[mm^3], 1.1[kg]). As the results of redesigning prototype, stable operation was realized . Semi-closed feedback control system using rotary encoders mounted on motors improved the positioning accuracy. Positioning accuracy of the gimbals mechanism was less than 0.6 [deg], and that of friction wheel mechanism was less than 0.2 [mm] in translation and 1 [deg] in rotation. *In vitro* experiment showed that no slip was observed under the existence of blood on the forceps with load of 2 [kg]. This manipulator will work in operating theater as a miniaturized surgical robot.

References

[1] R.H.Taylor, et al. A Telerobotic Assistant for Laparoscopic Surgery. *IEEE Engineering in Medicine and Biology*, 14(3):279–288, 1995.

[2] A.J.Madhani, et al. The Black Falcon : A Teleoperated Surgical Instrument for Minimally Invasive Surgery. In *Proc. of IEEE/RSJ IROS'98*, pages 936–944, 1998.

[3] Y.Kobayashi, et al. Small Occupancy Robotic Mechanisms for Endoscopic Surgery. In *Proc. of MICCAI2002*, pages 75–82, 2002.

[4] Mitsuishi,M., et al. Development of a remote minimally-invasive surgical system with operational environment transmission capability. In *Proc. of ICRA2003*, pages 2663–2670, 2003.

[5] T.Suzuki, et al. Development of master-slave robotic system for laparoscopic surgery. In *Proc. of The 5th International conference on Machine Automation (ICMA2004)*, pages 35–40, 2004.

[6] A.R.Lanfranco, et al. Robotic Surgery: A Current Perspective. *Annals of Surgery*, 239(1):14–21, 2004.

[7] M.Vollenweider, et al. Surgery Simulator with Force Feedback. In *Proc. of 4th International Conference on Motion and Vibration Control (MOVIC98)*, 1998.

[8] K.Ikuta et al. Virtual Endoscope System with Force Sensation. In *Proc. of MICCAI98*, pages 293–304, 1998.

[9] H.Yamashita, et al. Multi-slider Linkage Mechanism for Endoscopic Forceps Manipulator. In *Proc of IROS2003*, pages 2577–2582, 2003.

[10] K.Nishizawa, et al. Development of Interference-Free Wire-Driven Joint Mechanism for Surgical Manipulator Systems. *J. of Robotics and Mechatronics*, 16(2):116–121, 2004.

[11] T.Suzuki, et al. Development of a Robotic Laser Surgical Tool with an Integrated Video Endoscope. In *Proc. of MICCAI2004*, pages 25–32, 2004.

[12] T.Suzuki, et al. A new compact robot for manipulation forceps using friction wheel and gimbals mechanism. In *Proc. of CARS2002*, pages 314–319, 2002.

[13] Y.Katayama, T.Suzuki, et al. New compact robot for manipulating forceps using friction wheel and gimbals mechanism. In *Proc. of JSPE*, 2004, (in Japanese).

[14] J.Marescaux, et al. Transcontinental Robot-Assisted Remote Telesurgery: Feasibility and Potential Applications. *Ann. Surg.*, 235(4):487–492, 2002.

[15] http://www.zero-max.com/products/rohlix/rohlixmain.asp.

[16] J.L.Hefti, et al. Robotic Three-Dimensional Positioning of a Stimulation Electrode in the Brain. *Journal of Computer Aided Surgery*, 3(1):1–10, 1998.

Compact Forceps Manipulator Using Friction Wheel Mechanism and Gimbals Mechanism for Laparoscopic Surgery

Takashi Suzuki, Youichi Katayama, Etsuko Kobayashi, and Ichiro Sakuma

Institute of Environmental Studies, Graduate School of Frontier Sciences,
The University of Tokyo, 7-3-1, Hongo, Bunkyo-ku, Tokyo 113-8656, Japan
{t-suzuki, katayama, etsuko, sakuma}@miki.pe.u-tokyo.ac.jp
http://bme.pe.u-tokyo.ac.jp/index_e.html

Abstract. This paper reports evaluation of compact forceps manipulator designed for assisting laparoscopic surgery. The manipulator consists of two miniaturized parts; friction wheel mechanism which rotates and translates forceps ($62\times52\times150$[mm^3], 0.6[kg]), and gimbals mechanism which provides pivoting motion of forceps around incision hole on the abdomen ($135\times165\times300$[mm^3], 1.1[kg]). The four-DOF motion of forceps around the incision hole on the abdomen in laparoscopic surgery is realized. By integration with robotized forceps or a needle insertion robot, it will work as a compact robotic arm in a master-slave system. It can also work under numerical control based on the computerized surgical planning. This table-mounted miniaturized manipulator contributes to the coexistence of clinical staffs and manipulators in the today's crowded operating room. As the results of mechanical performance evaluation with load of 4 [N], positioning accuracy was less than 1.2 [deg] in pivoting motion, less than 4 [deg] in rotation of forceps, less than 1.2 [mm] in longitudinal translation of forceps. As future works, we will modify mechanism for sterilization and safety improvement, and also integrate this manipulator with robotized forceps to build a surgery assisting robotic system.

1 Introduction

Today, as a means of minimally invasive surgery, laparoscopic surgery is widely performed. Surgeons cut small holes on the abdomen to insert laparoscope and forceps, and conduct all operations inside the abdominal cavity. Small incisions damage patients much less than conventional laparotomy, and patients can get relief from postoperative pain or medication. This patient-friendly technique, however, is rather difficult and cannot be applied to all cases, mainly because the limited degrees of freedom (DOF) of forceps eliminate the dexterity of surgeons (Fig.1(a)). Surgeons must take special training for laparoscopic surgery.

Responding to these issues, surgery-assisting robotic manipulators are developed. Some of them are clinically applied and show their availability [1,2]. Those new systems have provided surgeons with technologically advanced hand skills,

J. Duncan and G. Gerig (Eds.): MICCAI 2005, LNCS 3750, pp. 81–88, 2005.

and enabled higher-quality and more precise operation, that could not be realized in the conventional laparoscopic surgery. Meanwhile, the large size of them caused problems. Some robotic systems require larger room and are difficult to install into conventional crowded operating theater. As the operation space above the patient's abdomen is occupied by the manipulator arms, clinical staffs have troubles to observe the patient and have danger of collision with manipulators. Thus, a new compact surgery-assisting robotic system is required [3].

We have developed a compact forceps manipulator using "friction wheel mechanism" (FWM) [4] and gimbals mechanism (Fig. 1(b)). In the former study, a prototype was manufactured, and feasibility was shown as a forceps manipulator [5]. At the same time, some problems emerged. The rotational speed of ultrasonicmotor varied depending on various factors, that is, the motor we adopted for actuation was unstable, being affected by temperature and load, so that the motion of forceps was also unstable under the open-loop controlling system [6]. In the recent presentation [7], we reported mechanical implementation of miniaturized ultrasonic motors with rotary encoder into the mechanically-modified prototype, and reported evaluation of basic performance using feedback control system. Positioning accuracy of the gimbals mechanism was less than 0.6 [deg], and that of friction wheel mechanism was less than 0.2 [mm] in translation and 1 [deg] in rotation.

In the former studies, the accuracy was measured as a static positioning device without load. Thus, in this study, we measured and evaluated static position accuracy with load of 4 [N]. In section 2, we introduce the configuration and mechanism of our compact forceps manipulator. Experimental apparatus and evaluation results are shown in section 3. We discuss the results of performance evaluation in section 4. Conclusions are presented in section 5.

2 System Configuration

We adopted following two mechanisms to realize four-DOF motion of forceps required in laparoscopic surgery(Fig.1(a)); "Friction wheel mechanism" (FWM) provides the rotation around the forceps shaft and translation along the shaft (number (1) and (2) in Fig.1(b)). Gimbals mechanism realizes the pivoting motion to determine the direction of the forceps (number (3) and (4) in Fig.1(b)). The dimension of the FWM is $62\times52\times150[mm^3]$ and the weight was 0.6[kg]. Those of gimbals mechanism are $135\times165\times300[mm^3]$ and 1.1[kg]. We mount this manipulator near the incision hole using multiple joint arm (ex. Iron intern$^{(R)}$ [8] or Point setter [9]). This is because mechanisms and actuators should be mounted near the operating field so that they require less torque or force [3].

Friction wheel mechanism (FWM) consists of three titled idle rollers and outer case (Fig. 2(a)). Three idle rollers around the forceps shaft travel spirally on the surface of shaft when outer case rotates (Fig. 2(b)) [10]. A couple of FWMs with opposite tilting angle (like right-handed screw and left-handed one) hold the forceps shaft(Fig. 2(c)). When they rotate in the same direction, the shaft held statically by rollers rotates around its longitudinal axis (Fig. 3(a)).

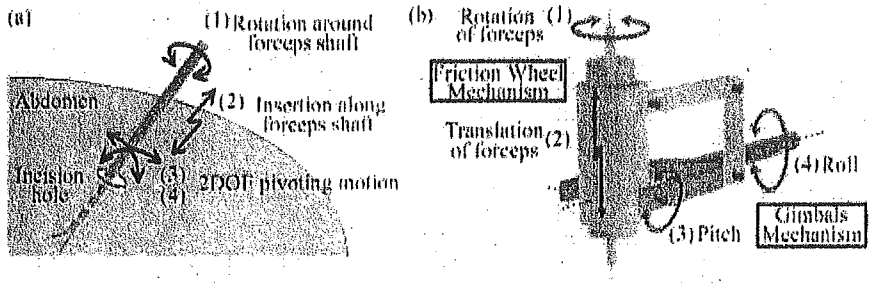

Fig. 1. System configuration, (a) In laparoscopic surgery, forceps have only four degrees of freedom: two for rotation(1) and insertion(2) of forceps, two for pivoting motion(3)(4) around the incision hole. (b) Friction Wheel Mechanism provides two motions of (1) and (2). Gimbals mechanism realizes the rotational motions of (3) and (4).

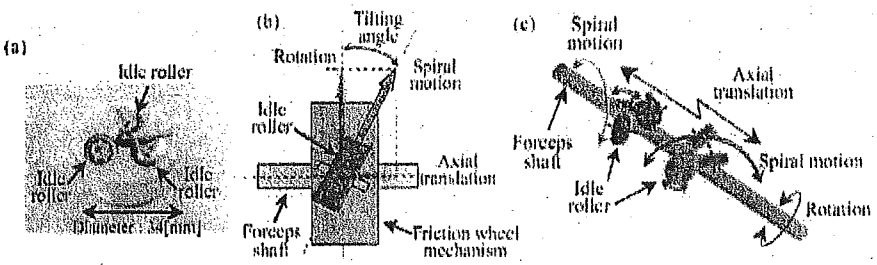

Fig. 2. Friction wheel mechanism, (a) a FWM has three rollers (arrow). (b) Rollers travel spirally on the surface of shaft. That motion can be divided into axial translation along the shaft and rotation around the shaft. (c) We combine two different spiral motions to realize rotation and translation.

Alternatively, when they rotate in the opposite direction, rollers travel on the shaft spirally and rotational motion is cancelled by rotational component of each spiral motion, so that forceps moves along its axis (Fig. 3(b)). The tilting angle was set at 30 [deg] in this study. We used hollow-shaft ultrasonic motors with rotary encoder (custom order, Fukoku, Japan) to drive the outer case of FWM for miniaturization of the system. The resolution of the rotary encoder was 0.2 [deg/pulse].

Gimbals mechanism provides pivoting motion, two rotational motions around the mutually-perpendicular axes. It is to be noted that pivot center of this manipulator is not located at the incision hole, but at the intersectional point of two axes. As for a surgery assisting robot for laparoscopic surgery, "remote center of motion (RCM)" mechanism should be mounted to bind the rotational center of manipulator at the incision hole (ex.[11,12]). However, as we reported in [5], it is not always necessary. This was because abdominal muscle under anesthesia gets flaccid and manipulator does not damage the abdominal wall by driving the

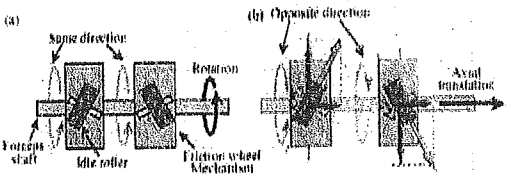

Fig. 3. Driving mechanism of forceps, (a) Rotation, (b) Translation

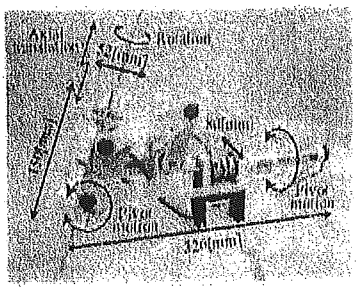

Fig. 4. New prototype

forceps. We used geared DC servomotors (ENC-185801, Chiba Precision Co.,Ltd, Japan) for actuation. The reduction gear ratio was 1/576. The resolution of the rotary encoder was 0.36[deg/pulse]. The prototype is shown in Fig. 4.

3 Evaluation Experiments

We conducted mechanical performance evaluation of our forceps manipulator. In the former studies, we conducted performance evaluation without any load [5,6,7]. Thus, in this study, we applied a load of 4[N], that was equivalent to the one third weight of Japanese male liver.

We measured working range and positioning accuracy of each axis (pitch and roll motions in gimbals mechanism, rotation and longitudinal translation of forceps in FWM) with load. Motion of manipulator was recorded using digital microscope (VH-7000C, KEYENCE, Japan), and working range and positioning

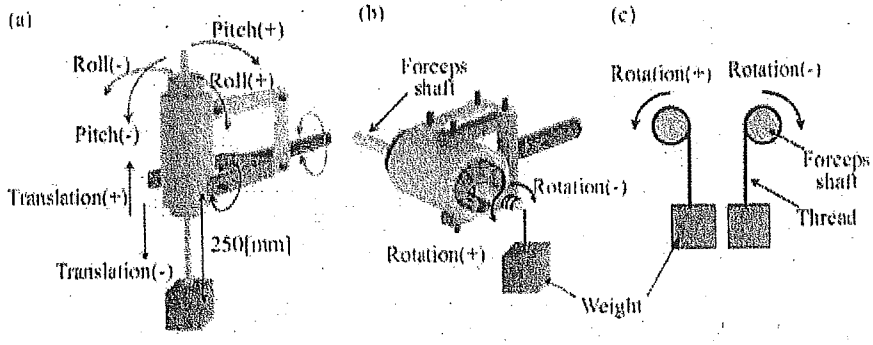

Fig. 5. Experimental setup, (a) Forceps were initially set in the vertical position to measure the motion of gimbals mechanism and the translation. Input direction is defined as shown here. (b) In the evaluation of rotation, forceps were set horizontally. (c) We measured the rotational positioning accuracy of forceps when forceps were pulling up the weight.

accuracy were measured by its accompanying utility software. Each measurement was repeated for twelve times. In order to reduce the measuring error, maximum and minimum values were eliminated, and the average and standard deviation of other ten values were calculated. Positive value in positioning error means that manipulator overruns beyond the input command, and negative means that it does not reach the goal. The definition of +/- input direction is shown in Fig. 5. As the initial setting, the forceps were set vertically in the evaluation of gimbals mechanism and translation of forceps (Fig. 5(a)), and horizontally in rotation (Fig. 5(b)). The distance between the weight and the center of gimbals mechanism was 250 [mm].

3.1 Gimbals Mechanism

Working range of gimbals mechanism was measured. No decrease of working range was shown (Table. 1). Positioning accuracy of the gimbals mechanism was measured at every 5 [deg] from −30 [deg] to +30[deg]. Measurement results are shown in Fig.6, comparing the results of evaluation without load [7]. Accuracy was less than 1.2 [deg] in pitch and roll motions.

3.2 Friction Wheel Mechanism (FWM)

As for the working range, FWM has no mechanical limitation, and the load did not limit the working range (Table. 1).

Before measuring the positioning accuracy, we evaluated the separation of rotation and translation. Because rotation and translation of forceps are generated by combining a couple of spiral motions, if each spiral motion differs from each other because of machining error, rotational error occurs in translation and translational error occurs in rotation [7,13]. Thus we measured the motion error beforehand and added compensation factor. When 45 [mm] translation command (that corresponds to 5 revolutions or 1800[deg] rotation of friction wheel) was input, forceps rotated 14.3 [deg]. This means that the difference of rotational traveling distance between FWMs is 14.3 [deg]. Thus we applied two coefficients; 1 - (14.3 / 1800) to longer traveling one, and 1 + (14.3 / 1800) to shorter traveling one.

Positioning accuracy of FWM was measured at every 45 [deg] from −180 [deg] to +180[deg] in rotation, and at every 20[mm] from −80 [mm] to +80[mm]

Table 1. Results of Working Range Evaluation

	Working Range	
	with load	w/o load
Pitch [deg]	−35.0 – +37.0	−35.0 – +37.0
Roll [deg]	± 180.0	± 180.0
Rotation [deg]	no limitation	no limitation
Translation [mm]	no limitation	no limitation

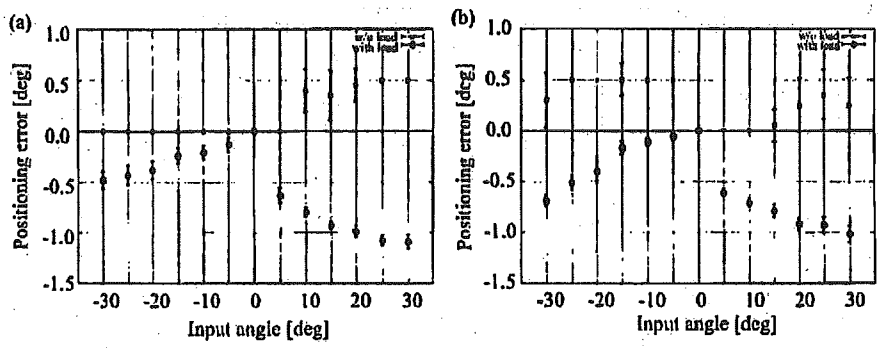

Fig. 6. Positioning accuracy of gimbals mechanism, (a) Pitch, (b)Roll

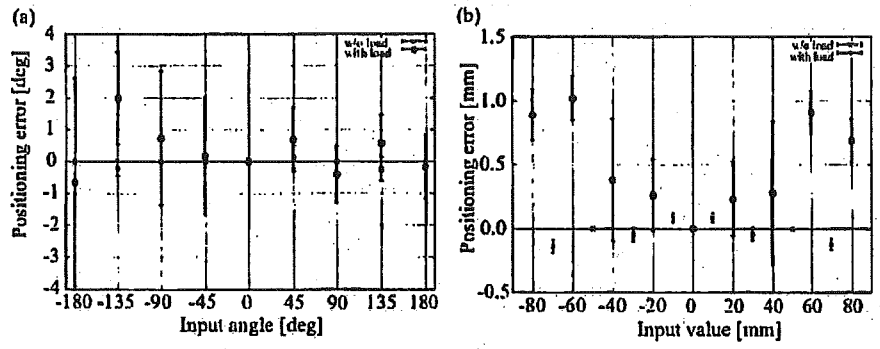

Fig. 7. Positioning accuracy of friction wheel mechanism, (a) Rotation, (b) Translation

in translation. The diameter of the forceps was 5 [mm], thus the torque applied by the weight was 10 [mNm]. Results are shown in Fig. 7. The accuracy was less than 4 [deg] in rotation of forceps, less than 1.2 [mm] in longitudinal translation.

4 Discussion

4.1 Working Range and Positioning Accuracy

Working range of gimbals mechanism and FWM did not affected by the load of 4 [N]. As for the roll motion of gimbals mechanism and rotation and translation of FWM, they have no mechanical limitation to realize wide range of motion. However, we can think mechanical limitation is desirable to ensure the safety in the case of malfunction. Some kind of safety mechanism should be implemented without wasting the advantages of gimbals mechanism and FWM.

As for the positioning accuracy of gimbals mechanism, it decreased as the input value increased. However, results showed the relative small standard devi-

ation and high repeatability, thus high positioning accuracy will be realized by adding offset into input command depending on the load.

Positioning accuracy of FWM also decreased, especially in the rotation of forceps. This would be because the friction force between idle roller and forceps shaft to hold the forceps is smaller than external force by the load. Though we used stainless steel for idle rollers and shaft from the viewpoint of future washing and sterilization in the current prototype, we have to consider other materials to strengthen the friction force.

4.2 Future Works

We have following plans as near-term future works.

1. We will measure the dynamic response characteristics with/without load. The dynamic characteristics must be known to drive this manipulator smoothly as a slave robotic arm in a master-slave system.

2. As a related work, we evaluated the tilting angle of idle rollers in FWM [15]. In that study, FWM with rollers of 45 [degree] tilting angle showed higher speed, torque and force, and did not show any decrease in the positioning accuracy, comparing with those of 30 [degree], those were used in this study. Thus we will replace the FWMs with new ones.

3. Sterilization-compatible mechanism should be implemented for the clinical application. We will use "separation method" that separates sterilized and non-sterilized part via transmission part [14].

5 Conclusion

In this study, we evaluated the compact forceps manipulator using gimbals mechanism and FWM. As the results of experiments applying 4[N] load, positioning accuracy of the gimbals mechanism was less than 1.2 [deg], and that of friction wheel mechanism was less than 4 [deg] in rotation and 1.2 [mm] in translation.

This manipulator can work as a compact robotic arm to manipulate various kinds of forceps, ex. wire-driven bending forceps [16], bending forceps using linkage mechanism [17], and laser surgical tool [18], or rigid laparoscope can be manipulated with this system. In other words, this manipulator can be a common platform for robotized forceps. Thus we are going to integrate various surgical instruments with this manipulator to use robotized sophisticated surgical equipments.

Acknowledgement

This work is partially supported by "Research for the Future Program (JSPS-RFTF 99I00904)" funded by Japan Society for the Promotion of Science, Electro-Mechanic Technology Advancing Foundation, "Research and Development of the Compact Surgical Robot System for Future Medical Care" funded by New Energy and Industrial Technology Development Organization (NEDO), and "Research on medical devices for analyzing, supporting and substituting the function of human body" funded by Ministry of Health, Labour and Welfare.

References

1. M.Hashizume, et al. Robotic Surgery and Cancer: the Present State, Problems and Future Vision. *Jpn.J.Clin.Oncol.*, 34(5):227–237, 2004.
2. A.R.Lanfranco, et al. Robotic Surgery: A Current Perspective. *Annals of Surgery*, 239(1):14–21, 2004.
3. Y.Kobayashi, et al. Small Occupancy Robotic Mechanisms for Endoscopic Surgery. In *Proc. of MICCAI2002*, pages 75–82, 2002.
4. M.Vollenweider, et al. Surgery Simulator with Force Feedback. In *Proc. of 4th International Conference on Motion and Vibration Control (MOVIC98)*, 1998.
5. T.Suzuki, et al. A new compact robot for manipulation forceps using friction wheel and gimbals mechanism. In *Proc. of CARS2002*, pages 314–319, 2002.
6. Y.Katayama, T.Suzuki, et al. New compact robot for manipulating forceps using friction wheel and gimbals mechanism. In *Proc. of JSPE*, 2004, (in Japanese).
7. T.Suzuki, et al. Compact Forceps Manipulator for Laparoscopic Surgery. In *Proc. of IEEE/RSJ IROS2005*, page accepted, 2005.
8. http://www.ironintern.com/amp/.
9. http://www.mitakakohki.co.jp/english/med_index.html.
10. http://www.zero-max.com/products/rohlix/rohlixmain.asp.
11. R.H.Taylor, et al. A Telerobotic Assistant for Laparoscopic Surgery. *IEEE Engineering in Medicine and Biology*, 14(3):279–288, MayJune 1995.
12. A.J.Madhani, et al. The Black Falcon : A Teleoperated Surgical Instrument for Minimally Invasive Surgery. In *Proc. of IEEE/RSJ IROS'98*, pages 936–944, 1998.
13. K.Ikuta et al. Virtual Endoscope System with Force Sensation. In *Proc. of MICCAI98*, pages 293–304, 1998.
14. J.L.Hefti, et al. Robotic Three-Dimensional Positioning of a Stimulation Electrode in the Brain. *Journal of Computer Aided Surgery*, 3(1):1–10, 1998.
15. T.Suzuki, et al. Improvement of compact forceps manipulator using friction wheel mechanism. In *The 1st Asian symposium on computer aided surgery*, page OR1, 2005.
16. R.Nakamura, et al. Multi-DOF Forceps Manipulator System for Laparoscopic Surgery - Mechanism miniaturized & Evaluation of New Interface -. In *Proc. of MICCAI2001*, pages 606–613, 2001.
17. H.Yamashita, et al. Handheld Laparoscopic Forceps Manipulator Using Multi-slider Linkage Mechanisms. In *Proc. of MICCAI 2004*, pages 121–128, 2004.
18. T.Suzuki, et al. Development of a Robotic Laser Surgical Tool with an Integrated Video Endoscope. In *Proc. of MICCAI2004*, pages 25–32, 2004.

原 著

脳外科用レーザ手術装置のための小型オートフォーカスシステムの開発

Development of a Compact Automatic-Focusing System for a Neurosurgical Laser Instrument

野口雅史[a], 青木英祐[a], 小林英津子[a], 大森 繁[b/c], 村垣善浩[c],
伊関 洋[c], 佐久間一郎[a]
[a]東京大学大学院新領域創成科学研究科, [b]テルモ(株)
[c]東京女子医科大学大学院先端生命医科学研究所先端工学外科

Masafumi Noguchi[a], Eisuke Aoki[a], Etsuko Kobayashi[a], Shigeru Omori[b/c], Yoshihiro Muragaki[c], Hiroshi Iseki[c], Ichiro Sakuma[a]
[a]Graduate School of Frontier Sciences, The University of Tokyo
[b]Terumo Corporation
[c]Faculty of Advanced Techno-surgery, Institute of Biomedical Engineering and Science, Graduate School of Medicine, Tokyo Women's Medical University

Abstract

In neurosurgery such as the treatment of glioma, it is very important to remove tumor as accurately as possible at the boundary between tumor and normal tissue in order to prevent the recurrence. To achieve this, we had proposed a robotic laser scanning system using a micro laser with wave length of 2.8 um. This micro laser is suitable to remove the tumor at the brain surface because of its strong absorption feature by water. It is necessary, however, to keep the distance between the laser probe and the target at its focal length. In this research, we developed an automatic-focusing system using a guide laser and a CCD camera. In addition, we performed some experiments for evaluation *in vitro* and an *in vivo* test with the laser ablation on a porcine brain. Results showed that accuracy of focusing largely depends on the condition of the brain surface. In the near future, we will improve our method so that it will not be affected by the condition of the brain surface.

Key words

Neurosurgery, Laser ablation, Automatic focusing, Medical robot, Brain tumor.

1. はじめに

原発性脳腫瘍の中でも神経膠腫は最も多くの割合を占める. 特に悪性の神経膠腫については, 手術による摘出, 薬物, 放射線治療などを駆使した総合的治療にも関わらず, 術後の平均生存率は 1 年程度とかなり低いものである. 脳腫瘍全国統計の悪性神経膠腫 6398 例によると, 全摘出, 95%以上摘出, 95%未満摘出した場合の 5 年生存率はそれぞれ, 40%, 22%, 10~15%であり, 腫瘍を全摘出することで患者の生存期間が大きく延びることが分かっている. しかし, 実際

＊東京大学大学院新領域創成科学研究科
〒113-8656 東京都文京区本郷 7-3-1 工学部 14 号館 722
masamasa@miki.pe.u-tokyo.ac.jp
受付 2004 年 8 月 6 日;採択 2005 年 1 月 5 日

には全症例中で全摘出といえるのはわずか 6~8%程度にすぎないという現状がある．これは，脳腫瘍と正常組織の境界を肉眼で正確に判断するのが困難であることに起因する．また場合によっては，腫瘍が脳の重要な機能を持った部位周辺に存在することもある．こういったケースでは，過度の摘出による機能障害の発生を防ぐため，腫瘍の腫瘍の除去を不完全にせざるを得ない．これも，腫瘍の全摘出を難しくする要因である．

そのため，術中MRIを用いた術中リアルタイムナビゲーションシステムや 5-Aminolevulinic-Acid (5ALA) を用いた術中リアルタイム計測システムを用いた治療が有効となる[1)-3)]．これにより腫瘍位置・形状が精確に把握できるようになる．しかし，これらのシステムにより腫瘍の位置を同定できたとしても，正常部位との境界に残ったわずかな残存腫瘍を，人間の手で過不足なく精確に除去するのは困難である．

そこで，この残存腫瘍の精確な除去法として，波長2.8μmのマイクロレーザを用いる方法が研究されてきた[4)]．このマイクロレーザは，CO_2やYAGレーザに比べ水による吸収が大きいため，生体に照射した場合，効果の及ぶ範囲が組織表面のごく表層に限られる．よって正常組織を傷めることなく，わずかに残った腫瘍部位のみを取り除くのに適している．また，石英ファイバを通すことができるため，装置本体の小型化も容易である．さらに，このマイクロレーザは焦点深度が±1mm程度であり，この範囲のみ蒸散効果が得られるため，安全性の面で非常に優れている(Fig. 1)．一方，蒸散により脳腫瘍を精確に除去するには，複雑な形状をした脳表面に対し，治療対象面とレーザ先端との距離を一定に保つ必要がある．また，プローブの走査速度によって脳表へのエッチングの深さが変化するという性質もある[5)]．人間の手でこれらを制御するのは困難であり，この焦点深度内へのフォーカシングおよび適切な走査スピードでの蒸散を自動で行なう装置が必要となる．

そこで本研究では，マイクロレーザによる治療中，脳表層のエリアを走査する動きに追従することが可能なフォーカシング装置の開発を目的とする．

本稿では，フォーカスシング方式の説明，製作した試作機に関する性能評価実験，ブタを用いた *in vivo* 動作実験の結果を報告する．また，これらの結果より現状の問題点を考察し，今後の展開について述べる．

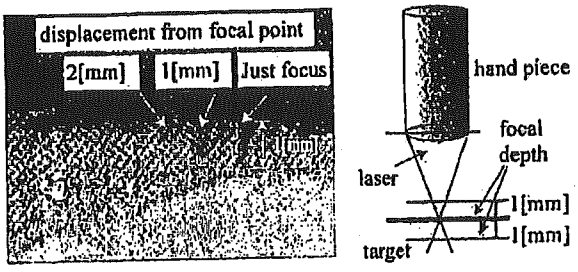

Fig. 1 Focal depth of the micro laser.

2. 方法

2．1 要求仕様

本研究において製作する手術装置の要求仕様を以下のように定める．

A) フォーカスシング精度±0.5mm 以内
B) 非接触によるフォーカシング
C) 手術場環境での照明下(明視下)でのフォーカシング
D) レーザの送り速度(2mm/s)に対する充分な追従性
E) 小型軽量

マイクロレーザの焦点深度は±1mm であるが，要求仕様には±0.5mmを設定する．脳外科の狭い術野に対して，術者のアプローチを妨げず，術中に装置を動かす際の負担を軽減するために，小型軽量である必要がある．

2．2 システム構成

システムの概観を Fig. 2 に示す．本システムでは，ガイドレーザと計測用小型 CCD カメラを用いた変位計測法によりフォーカスシングを行なう．CCD カメラによって撮影した画像を画像処理ボード(㈱日立ハイコス製，IP5000)により取得し，ガイドレーザスポットの重心座標を算出する．この重心座標から，Z 軸方向の補正量を求め，モーションコントロールボード(Interface 社製，PCI7208)へ指令を送り，直動ステッピングモータを用いた位置制御によりフォーカシングを行なっている．

2．3 装置

装置の試作機を Fig. 3 に示す．ただし，装置上部に取り付ける X,Y 方向走査用自動ステージ，マイクロレーザについては取り外した形になっている．フォーカスの駆動には，小型の直動ステッピングモータ(オリエンタルモーター社製，CPL28T2B-01)を使用している．